International Journal of Advances in Engineering and Management (IJAEM)
Volume 4, Issue 5 May 2022, pp: 2243-2258 www.ijaem.net ISSN: 2395-5252

Numerical Analysis of the Double-Ramp Compression Geometry Used in a Scramjet Inlet

Saurabh Kumar, Mritunjaya Verma, Shivansh Awasthi.
Student, Shri Ramswaroop Memorial college of Engineering and Management, Lucknow, Uttar Pradesh
Corresponding Author: Saurabh Kumar.

Submitted: 20-05-2022 Revised: 28-05-2022 Accepted: 30-05-2022

ABSTRACT:Essentially, our primary field of investigation is the fluid mechanics aspect. The double shock penetration principle of scramjet engines makes it a one-of-a-kind entity in supersonic region of rocket and missile lift-off. This one-of-a-kind idea is solely accountable for the range of Mach numbers that it can reach.
Among the many research areas in scramjet flow study, the evaluation of aerodynamic performance of the boundary-layer transition on the forebody and complex shockwave/boundary-layer interactions (SBLI) in the intake have received special attention. Both problems are critical for understanding and modelling supersonic combustion with resultant high engine thrust.

KEYWORDS: Numerical analysis, Scramjet, Ramp angles, Mach number, Isolator region, Shockwave angles, Reynolds-Averaged Navier-Stokes Equation, Stagnation Pressure Ratio.

I. INTRODUCTION

A scramjet (supersonic combustion ramjet) is a type of ramjet air-breathing combustion jet engine. Scramjet is essentially an enhanced version of a turbojet engine that operates at greater Mach numbers. Its lowest limit is set at 6, while the higher limit has yet to be determined. A ramjet engine, on the other hand, works at speeds ranging from 3 to 6 Mach numbers. Ramjet engines are incapable of working at greater speeds, which is why the concept of scramjets was invented and has proven to be a huge success.

The turbojet is an air breathing jet engine that is commonly seen in airplanes. It is made up of a gas turbine and a propelling nozzle. An air intake, a compressor, a combustion chamber, and a turbine are all part of a gas turbine (that drives the compressor). The compressed air from the compressor is heated in the combustion chamber by burning fuel and then allowed to expand via the turbine. The turbine exhaust is then expanded in the propelling nozzle and accelerated to high speeds to generate thrust. During the late 1930s, two engineers, Frank Whittle in the United Kingdom, and Hans von Ohain in Germany, independently developed the concept into functional engines.

Turbojet engines typically run at Mach numbers ranging from 0 to 3. For years, they were extremely successfully operating very well and producing the intended result. However, their substantial constructions add to the overall weight of the system.

A ramjet, also known as a flying stovepipe or an athodyd (aero thermodynamic duct), is a type of air breathing jet engine that compresses incoming air using the engine's forward motion rather than an axial or centrifugal compressor. Ramjets cannot move an airplane from a stop because they cannot create thrust at zero velocity. Due to this, a vehicle powered by ramjet requires an aided take-off, like a rocket assist, to propel it to a speed where it thrust can be created. Ramjets perform best at supersonic speeds of roughly Mach 3 (2,300 mph: 3,700 km/h). This engine can reach speeds of up to Mach 6 (4,600 mph: 7,400 km/h).

A scramjet (supersonic combustion ramjet) is a ramjet airbreathing jet engine with supersonic combustion. A scramjet, like a ramjet, relies on high vehicle speed to compress the incoming air forcefully before combustion (hence the name ramjet), but unlike a ramjet, which uses shock cones to decelerate the air to subsonic velocities before

International Journal of Advances in Engineering and Management (IJAEM)
Volume 4, Issue 5 May 2022, pp: 2243-2258 www.ijaem.net ISSN: 2395-5252

combustion, a scramjet has no shock cone and slows the airflow using shockwaves produced by its ignition source in place of a shock cone. As a result, the scramjet can run at exceptionally high speeds while being efficient.

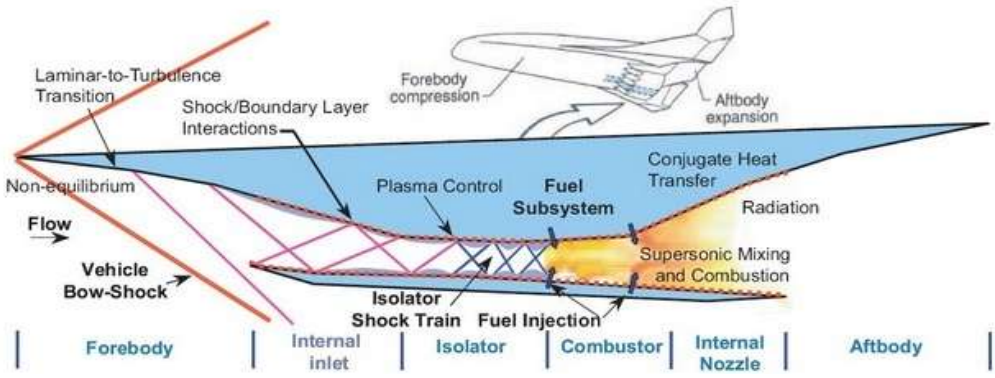

Descriptive diagram of Scramjet engine

The heat addition caused by the combustion process happens in a supersonic airflow relative to the engine of a scramjet. In terms of ramjets, a scramjet depends on a faster vehicle flying speed to compress and slow the entering airflow before combustion.

The airflow in a scramjet remains 'supersonic' throughout the engine cycle, whereas the airflow in a ramjet decelerates to 'subsonic' speeds. This allows the scramjet to run at higher speeds and with more efficiency.

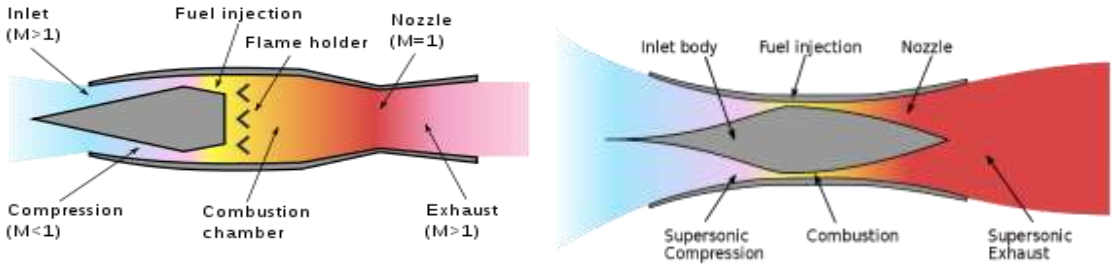

Schematic diagrams of (a)ramjet engine and (b) scramjet engine

II. LITERATURE REVIEW

Scramjet engines have a vast history. First concept that came on paper was in 1964. The concept came up in year between 1950s and 1960s. The concept was totally based on the inlet portion of the engine as rest is same as that of ramjet engine. Scramjet (supersonic combustion ramjet) engine, as the name suggests, is an upgradation of ramjet engine which developed in 1913 by French inventor Rene Lorin.

But ramjets are not capable of operating at more higher speeds. So, there was a need to change or modify the aerodynamic design of the inlet to compress the air and work at supersonic speeds i.e., Mach number 5 to 10. Now the concept of scramjet engines came in early 1950s. By Alexander Kartveli and Antonio Ferri.

1950s-1960s

In November 1964, Antonio Ferri successfully demonstrated a scramjet eventually producing 517 pounds force i.e., 2.30 kN in which about 80% of his goal was completed but was not able to propose his theory. In 1964 itself, Fredrik Sybille, and Gordon L. Dugger submitted a patent application for a supersonic combustion ramjet engine based on Billig's PHD thesis.

But before all these works of intellectuals on scramjet engine, the concept of possibility of adding heat directly to a stream operating on supersonic speeds by means of a standing wave had been proposed by Roy as early 1946. He proposed this theory and was taken in consideration in 1960s to apply on scramjet engines. Later, in 1959, Nicholls et al.7 demonstrated stabilized detonation waves in supersonic hydrogen air streams. A joint British and Australian team from UK defence company Qinetic and the University of Queensland were the first group to demonstrate a scramjet working in an atmospheric test.

International Journal of Advances in Engineering and Management (IJAEM)
Volume 4, Issue 5 May 2022, pp: 2243-2258 www.ijaem.net ISSN: 2395-5252

At first, work on two engines took place, NASA HRE (Hypersonic Research engine) and Russian device created by group E.S. Schettino. These engines used very bulky and big compressors which were very much like turbojet engines which was the main disadvantage of turbojet engine (it's bulkiness). In NASA HRE, fuel to cool the walls of combustion chamber was hydrogen. On the other hand, Russian device used kerosene. In 1954, an experimental rocket propelled aircraft equipped with rocket engine was developed named as X-15 which was crashed and damaged. After this incident, it was decided to restore the X-15 with podded NASA HRE and named as X-15A-2. After testing, it was made to experimental flight which failed as the walls of the aircraft were heated up to 1480 ℃. This led to burning of aircraft shell and produced holes on the surface.

Then later, new design proposed was very much simple and effective as well. Here, the engine was placed just after the head shock wave. Therefore, here necessary compression is done by the forward motion of the aircraft carrier. Also, the design was made to be very thin so there was very much less drag induced in comparison to hypersonic aircraft. But this design failed due to its bulky configuration which involved a powerplant, rocket engine and the ramjet engine. This type of design was created in USA between 1985-1994 names as NASP (National Aero-Space Plane). The new NASA program "Hyper-X" (continuation of NASP) proposed to create a small hypersonic aircraft which was hydrogen fuelled scramjet. To apply this design, aircraft X-43A was created which was to achieve speed above Mach number 7 (approximately 8000 km/h) at an altitude of 30,000 m or more. Three models of these type aircrafts were made. Its flight lasted just for 11 sec above Pacific Ocean. But the other two successfully completed the program. Second flight X-43A took off on March 27, 2004. Then on November 16, 2004, third flight set a speed of 11.850 km/h.

In 2002, Hy Shot hypersonic aircraft was launched. It was lifted by Terrier-Orion Mk70 to a height 300km and dropped. On reaching the speed of 7.5 M, measuring process of scramjet engine begins. This aircraft lasted 6 seconds.

In 2009 to 2012, flight test was carried out under the HiFiRE program. This apparatus consists of an air inlet (two wedges) and scramjet chamber relative to symmetry plane of the apparatus. Fuel used was a surrogate mixture of ethylene, methane, and heptane. In the experiment, the pressure distribution on the chamber wall and the Mach number were measured. This experimental setup was located at NASA Langley.

The scramjet engine is the key to airbreathing hypersonic flight. Because of the energy limitations of currently available fuels, the scramjet is unlikely to provide efficient propulsion all the way to orbital speeds.

The unexpected complexities of scramjet combustion and combustor–inlet interactions, have frustrated progression the past 40 years. Indeed, it has taken the propulsion community over 30 years, since the conception of the engine, to achieve a successful flight test.

Y. Yao, D. Rincon, and Y. Zheng: - Shock induced separated flow inside a scramjet intake configuration has been studied by using a computational fluid dynamics approach of solving the Reynolds-averaged Navier- Stokes equations. At Mach 7 incoming flow and unit Reynolds number of 4.0E+6, two different intake geometries have been studied, i.e., sharp and rounded leading edges. Turbulence model created more difference than leading edges. Furthermore, turbulence model has resulted in quite similar wall pressure coefficient distribution, but its impact is significant on flow separation bubble. Large flow separation will lead to significant blockage of intake flow; thus, it is necessary to modify the expansion shoulder geometry to reduce large flow separation.

First, inlet designer should be careful about the sidewall compression that causes ramp shock to bend more upward and if the location of the cowl lip is not changed, there will be more occurrence of mass ow spillage.

Geometry-Due to the geometry of the scramjet engine, internal compression inlet generates a high amount of drag and it is not very easy to integrate the inlet with the whole vehicle. And the design of the internal compression inlet is rather complicated because of complex flow field structure and the need for variable geometry to establish stable flow.

Another important feature of an inlet is the number of ramps as it determines the flow field structure through the inlet and will in turn affect the overall compression ratio and the efficiency of the inlet.

It takes time for the combustion process to finish. Moreover, flow through the combustor moves at hypersonic speed. Therefore, there is a need of a specific length for a complete combustion

International Journal of Advances in Engineering and Management (IJAEM)
Volume 4, Issue 5 May 2022, pp: 2243-2258 www.ijaem.net ISSN: 2395-5252

process that will in turn determine the combustor length. Since the increase of the combustor length leads to more drag and heat load is placed upon the structure of the aircraft, short combustor is required. Increase of the combustor length leads the dramatic decrease of the overall performance of the aircraft. The flow to the combustor needs to reach certain value of pressure and temperature to achieve this goal.

The temperature of the air increases considerably relative to the free stream when the air is slowed down through the inlet. In the case of temperature being too high, some portion of oxygen and nitrogen in the air may be dissociated and some portion of the combustion product remains unformed. During the rapid expansion process through the nozzle, there is not enough time for the atoms in the air to recombine utterly, therefore portion of the energy received through the combustion process is not converted into thrust, which results in the decrease of the efficiency of the scramjet engine.

The capability of operating over a wide Mach number range without the use of variable geometry (moving cowl, rotating door), is the biggest challenge in scramjet inlet design.

III. EXPERIMENT

For the purposes of this project, we will consider the purely inviscid interaction, even though we acknowledge that the real flow will not look like this. A schematic representation of the problem is presented in Figure 2.1. The angles θ_1 and $\theta_2$are Ramp angles at which we are going to study the flow. β1 and β2 are shockwave angles formed due to incoming free stream air.

The wavelike structures that are formed result from this interaction should appear something like what is sketched in the given figure. Shock will be generated from both the compression corners, and these shocks will merge to form a single shock. Shocks are indicated in the schematic in blue. The additional wave that are formed from the triple point may be an expansion wave or a shock, depending on the flow configuration.

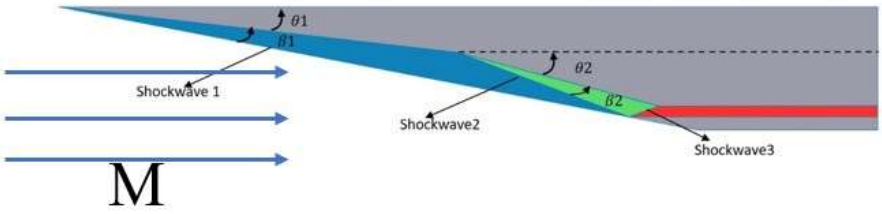

Schematic representation of the problem.

We are tasked to find the change in flow behaviour against the change of ramp angles:

i. Temperature difference in blue, green, and red zone.

ii. Mach number in blue, green, and red zones and Pressure loss in the red zone.

We have taken a standard model of a scramjet with a specified dimension, keeping it as our reference we have then varied the ramp 1 and ramp 2 angles along with that we have also varied the ramp lengths wherever necessary keeping rest of the geometrical parameters fixed. So, we have created total 4 models out of which the 1st model is the standard model with code name "XY", 2nd model is given the code name "R1-8" in which $\theta_1$is 8 degree, 3rd model is given the code name "R2-18" in which θ_2 is 18 and at last we have "R1-8_R2-18" which has the θ_1= 8 and θ_2=18.A more detailed specification is given below with figure and table containing all the dimensions.

Steps followed for creation Project methodology

1) Model Generation

Length and Width are common for all geometries.

International Journal of Advances in Engineering and Management (IJAEM)
Volume 4, Issue 5 May 2022, pp: 2243-2258 www.ijaem.net ISSN: 2395-5252

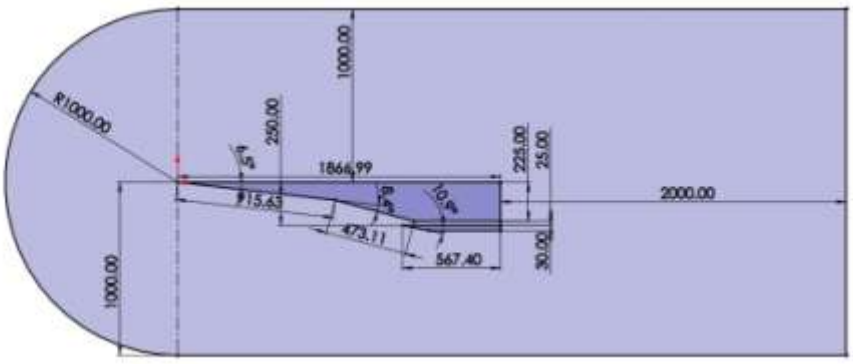

XY plane Inlet surface geometry(standard).

Dimensions XY plane inlet surface geometry

Length of R1	915.63mm
Length of R2	473.11mm
Angle of R1	6.5°
Angle of R2	14.9°
Total length	1866.99 mm
Total width	225.00 mm

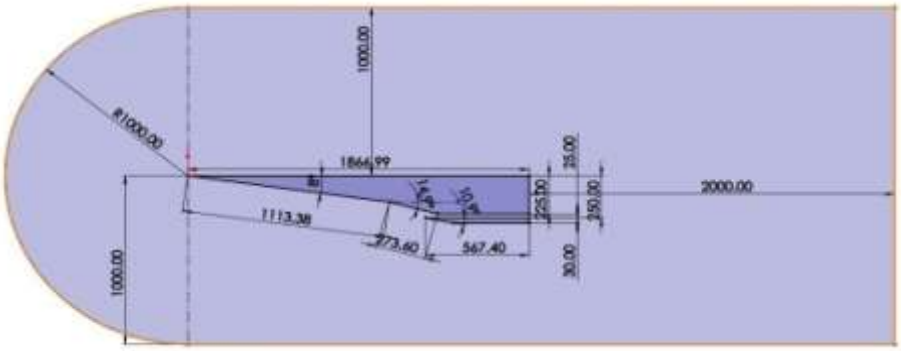

Inlet surface geometry R1-8

Dimensions XY plane inlet surface geometry R1-8

Length of R1	1113.38 mm
Length of R2	273.60 mm
Angle of R1	8.0°
Angle of R2	14.9°
Total length	1866.99 mm
Total width	225.00 mm

International Journal of Advances in Engineering and Management (IJAEM)
Volume 4, Issue 5 May 2022, pp: 2243-2258 www.ijaem.net ISSN: 2395-5252

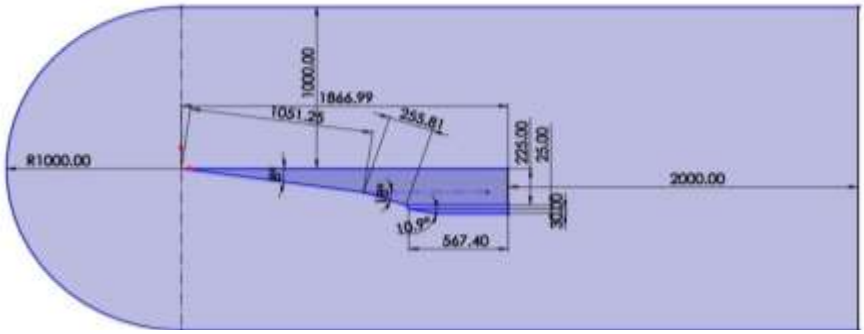

Inlet surface geometry R1-8_R2-18

Dimensions XY plane inlet surface geometry R1-8_ R2-18

Length of R1	1051.25 mm
Length of R2	255.81 mm
Angle of R1	8.0°
Angle of R2	18.0°
Total length	1866.99 mm
Total width	225.00 mm

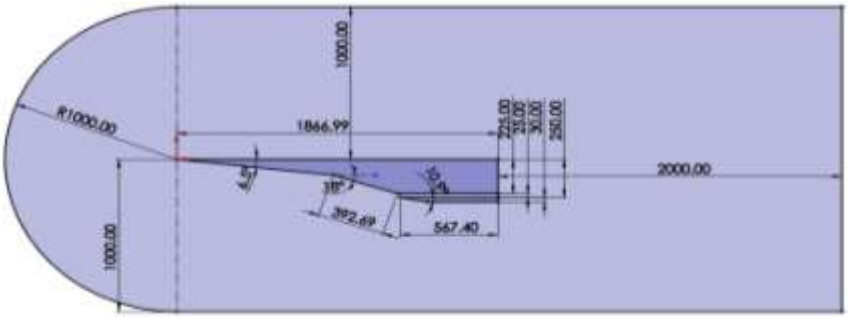

Inlet surface geometry R2-18

Dimensions XY plane inlet surface geometry R2-18

Length of R1	915.63 mm
Length of R2	392.69 mm
Angle of R1	6.6°
Angle of R2	18.0°
Total length	1866.99 mm
Total width	225.0 M

2) Mesh generation:

Mesh showcased below is for the first model only, other meshes are also like it with same mesh properties.

i. Mesh size:

Cells- 134676.

Faces- 202917.

Nodes- 68240.

ii. Mesh quality:

Cell Type- Tri Cell.

Minimum orthogonal quality-0.68913972.

Maximum aspect ratio- 3.9364979.

International Journal of Advances in Engineering and Management (IJAEM)
Volume 4, Issue 5 May 2022, pp: 2243-2258 www.ijaem.net ISSN: 2395-5252

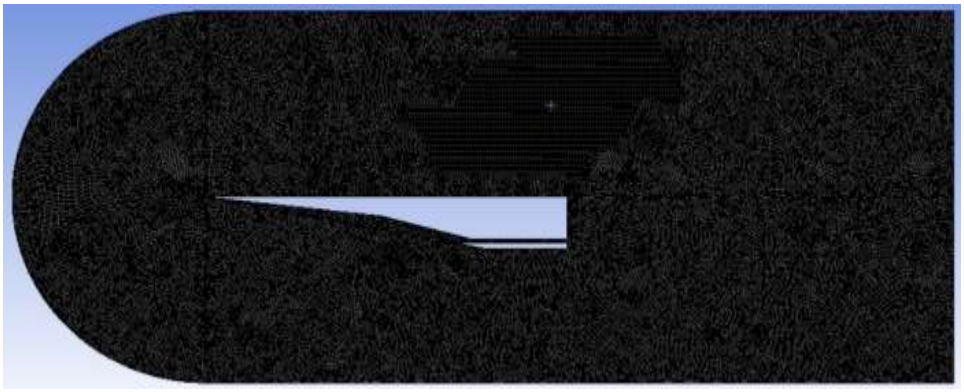

Mesh

3) Analysis performed on CAD model:

i) The computations are performed on Ansys to solve Reynolds-Averaged Navier-Stokes (RANS) in 2D using K-omega SST model.

ii) Free stream conditions area supersonic far field and hindered by solid CAD model.

iii) Then calculations are performed for 600 iterations till convergence is achieved.

Free stream conditions.

Pressure (Pa)	**Temperature (K)**	**Mach Number**
2806.2	220.7	5
1986.8	224.8	6
1459.8	229.3	7
1117.9	233.3	8
883.3	236.9	9
714.3	240.2	10

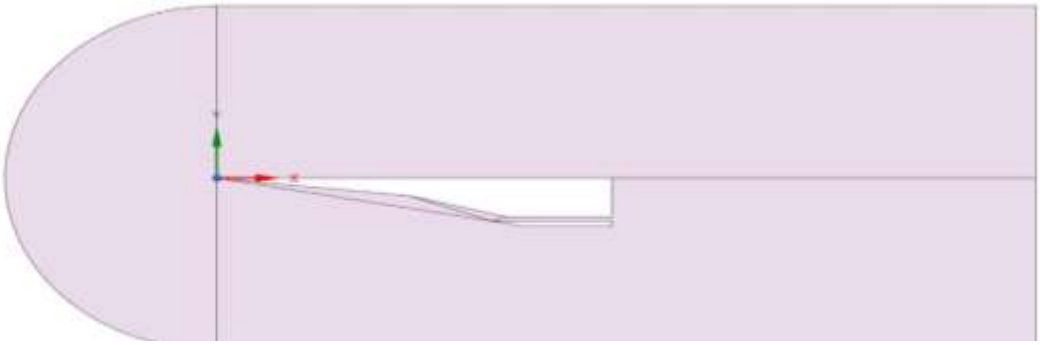

Far field

Fairfield dimensions

Fairfield radius	1000.00 mm
Fairfield length	3866.99 mm
Fairfield breadth	2000.0 M

1) Resultsare calculated by comparing parameters mentioned in the project objective and final remark will be given.

International Journal of Advances in Engineering and Management (IJAEM)
Volume 4, Issue 5 May 2022, pp: 2243-2258 www.ijaem.net ISSN: 2395-5252

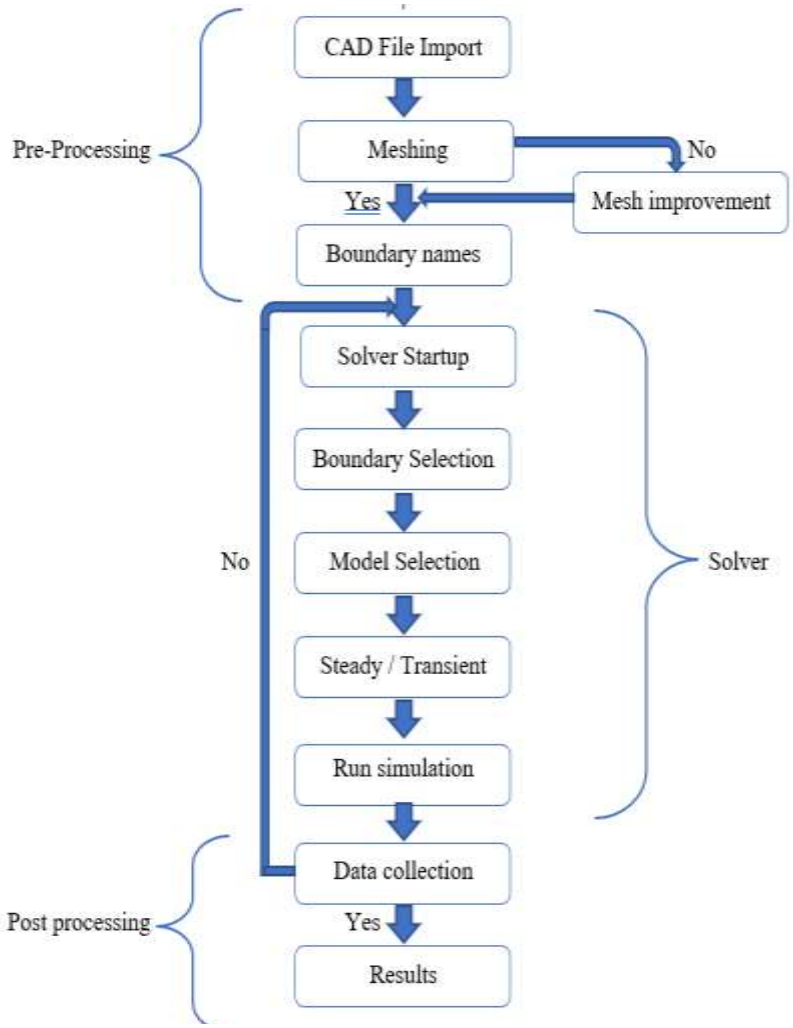

Process flow chart.

IV. NUMERICAL ANALYSIS OF SCRAMJET

The whole project is predicted on the compressive flow equation and the therefore law of gas dynamics the equation that we will be exploiting to outline and do the numerical study is Reynolds-Averaged Navier-Stokes (RANS). To ease out our calculation we will be representing all our data with help of MATLAB software.

Further will design a wall double ramp modal of the scramjet engine on Ansys and showcase the flow simulation.

As we have mentioned in project objective that we will be focusing our study on doing analysis of the double ramp at different angles thereby analysing the shock interaction on the side walls and the ramps.

Solution will be obtained using RANS equations keep inviscid boundary conditions.

The Reynolds-averaged Navier–Stokes equations (RANS equations) comes within the class of time-averaged equations of motion for fluid flow. The thought behind the equations is Reynold's decomposition, whereby an instantaneous quantity is decomposed into its time-averaged and fluctuating quantities, and concept first proposed by Osborne Reynolds. The RANS equations are primarily utilized in to describe in the case of turbulent flows. These equations are used with approximations based on knowledge of all required properties of flow turbulence to administer approximate time-averaged solutions to the Navier–Stokes equations. In the case of a stationary flow of an incompressible Newtonian fluid, these are the equations which can be describes and written in Einstein notation in Cartesian coordinates as:

International Journal of Advances in Engineering and Management (IJAEM)
Volume 4, Issue 5 May 2022, pp: 2243-2258 www.ijaem.net ISSN: 2395-5252

$$\rho\frac{\partial U_i}{\partial t}+\rho\frac{\partial}{\partial x_j}(U_iU_j)=-\frac{\partial P}{\partial x_i}+\frac{\partial}{\partial x_j}(2\mu S_{ij}-\rho\overline{u_i'u_j'})$$

Reynolds-averaged Navier–Stokes

The change in mean momentum of a fluid element is represented owing to the unsteadiness in the mean flow as well as convection by the mean flow, at the left-hand side of this equation. This variation is balanced by the mean body force, the isotropic stress due to the mean pressure field, the viscous stresses, and apparent stress due to the fluctuating velocity field, generally called to as the Reynolds stress. This nonlinear Reynolds stress term requires extra modelling to close the RANS equation for solving. This has led to the creation of many different turbulence models. The time-average operator in the equation is a Reynolds operator.

To capture turbulent flow conditions the K-omega model is one of the most used. The K-omega model belongs to the family of Reynolds-Averaged Navier-Stokes (RANS) family of turbulence models where all the effects of turbulence are modelled.

K-omega: It is a two-equation model. It means in addition to the conservation equations, it solves two transparent equations (PDEs), which account for the history effects like convection and diffusion of turbulent energy. The two transported variables are turbulent kinetic energy(K), which determines the energy in turbulence, and specific turbulence dissipation rate(ω), which determines the rate of dissipation per unit turbulent kinetic energy. Ω is also called to as the scale of turbulence.
There exist different variations of the k-omega model such as standard k-omega, baseline k-omega, k-omega SST, etc., each with certain modifications to perform better under certain conditions of the fluid flow.

K-Omega SST: SST stands for shear stress transport. K-omega SST provides a better prediction of flow separation than most RANS models and account for the transport of theprincipal shear stress in adverse pressure gradient boundary layers. It is most used model in the industry given its high accuracy to expense ratio.
Some disadvantages of it are that the SST model produces some large turbulence levels in regions with large normal strain, like stagnation regions and regions with strong acceleration. This effect is much less pronounced so than with a normal k-epsilon model though.

K-epsilon model: In Computational Fluid Dynamics the most common model used is K-epsilon for the simulation of mean flow characteristics for turbulent flow conditions. K-epsilon model focuses on the mechanisms that affect the turbulent kinetic energy unlike earlier models. The K-epsilon model is usually useful with free shear layer flows with relatively small pressure gradients. K-epsilon is best suited for flow away from the wall, say free surface flow region, whereas K-omega model is best suited for near the wall flow region, where adverse pressure gradient develops.

Mathematical Representation of k-omega:
The turbulent energy k is given by:

$$k=\frac{3}{2}(UI)^2$$

where "U"called mean flow velocity, and "I"know as turbulence intensity. The turbulence intensity gives the level of turbulence and can be defines as follows:

$$I=\frac{u'}{U}$$

where u' is defined as the root-mean square of the turbulent velocity fluctuations, given as:

$$u'=\frac{1}{3}\left(u'_{x^2}+u'_{y^2}+u'_{z^2}\right)=\sqrt{\frac{2}{3}k}$$

The turbulent viscosity v_t is calculated as:

$$v_t=\frac{k}{\omega}$$

V. RESULTS

For any Mach number& θ, any of the two cases are possible:

1) Two solutions
a) Weak shockwave occurs at usual and low β angles.
b) Strong shockwaves occur at high β angles.
2) No solutions
a) For a given Mach number, there is a maximum flow deflection angle $\theta_{max}$for which an attached shock is possible.

International Journal of Advances in Engineering and Management (IJAEM)
Volume 4, Issue 5 May 2022, pp: 2243-2258 www.ijaem.net ISSN: 2395-5252

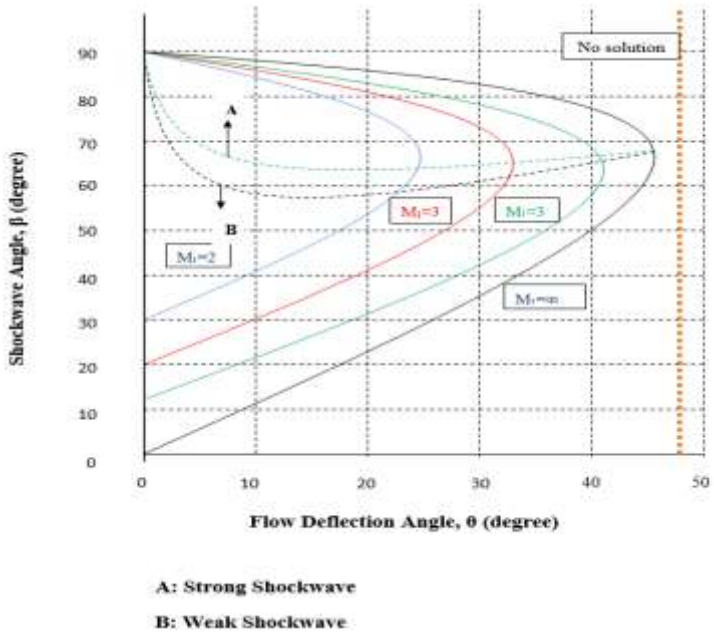

Shockwave angle vs Flow deflection angle

As mentioned in chapter 2 we have used four separate models with different dimensions with each given a special code. The following results are explained using those codes after performing the analysis, the following graphs have been plotted to showcase describe the flow behaviors. We will be discussing both the graphs one by one.

The first graphs are Stagnation pressure ratio vs Mach number graph. Talking about stagnation pressure ratio. It is the pressure ration between the free stream stagnation pressure to the stagnation pressure at the red region i.e., the region before the isolator region. This ratio shows the percentage of air that has compressed and entered through inlet, higher the value better will be the model. Data table is attached below the graph which show stagnation pressure ratio for each model from Mach 5 to Mach10.

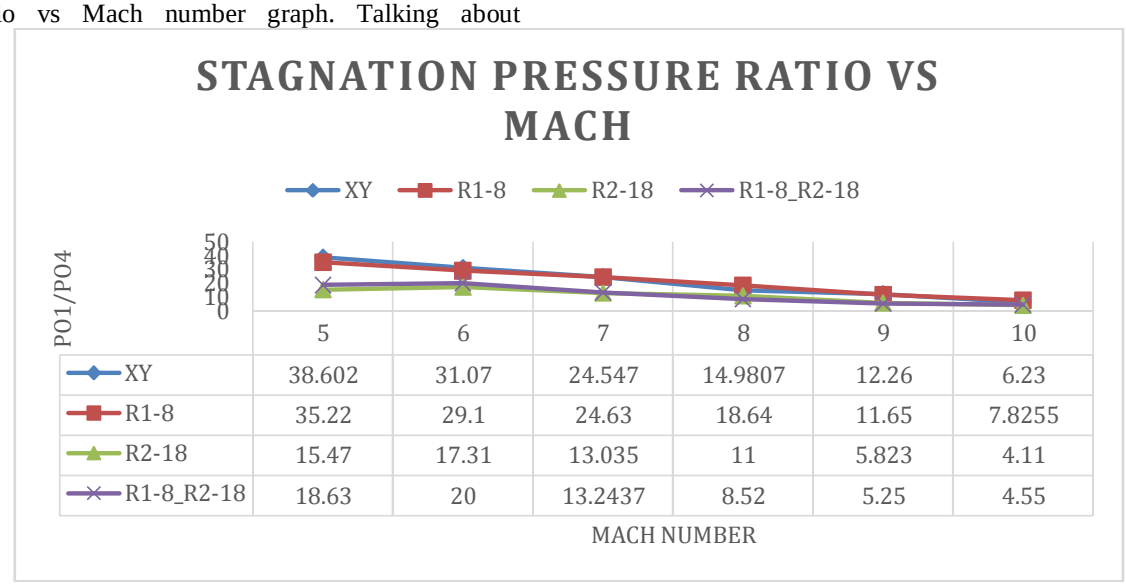

Stagnation Pressure ratio vs Mach.

International Journal of Advances in Engineering and Management (IJAEM)
Volume 4, Issue 5 May 2022, pp: 2243-2258 www.ijaem.net ISSN: 2395-5252

As we can see that the standard XY model has the maximum stagnation pressure ratio than the other model. First thing that we must understand is that, as the speed increases the flow condition changes thus the amount of air entering through inlet reduces. Thus, a model which has a consistent stagnation pressure ratio or shows result somewhere near to the standard model, will be considered as a good model. So, to understand this in depth we will compare and discuss each model separately with the standard model.

R1-8: This is the only model which at every free stream condition matches the results of the XY model and as the Mach number crosses the value of 8 it surpasses the standard model results, which means that at high Mach numbers more compressed air is reaching the isolator region.

R2-18 & R1-8_R2-18: Both models are not performing that efficiently as we can see the stagnation pressure ratios percentage are highly low as compared to the standard model and keeps on decreasing as Mach reaches 10.

Now we will see the 2nd graph, which is the Stagnation pressure ration vs Model.

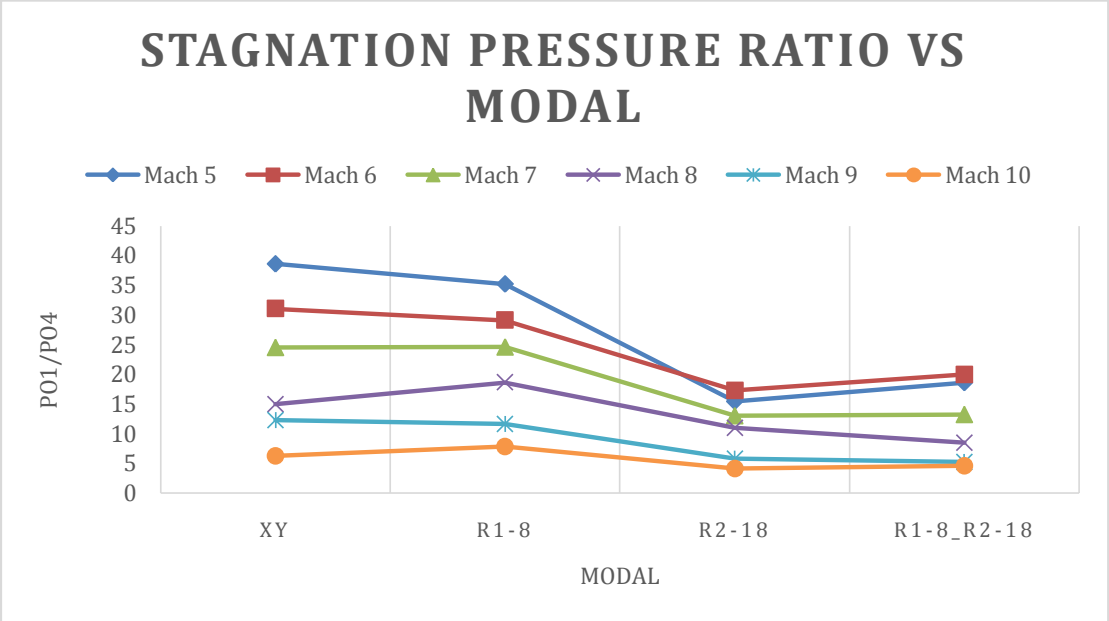

Stagnation Pressure ratio vs Model.

This graph gives us a clearer picture of stagnation pressure ration variation for each model. We can see that though the standard model initially had higher value of ratios and is very much close to the R1-8 model, yet the consistency is much better in the R1-8 model, that means there will be no sudden loss in the pressure or air flow in the combustion chamber. Thus, the combustion will not be hindered at higher Mach values. While the other 2 models are not performing that great and the main reason for them not performing are discussed later.

Advantages of R1-8 model: As you can see from the figure (inlet pressure geometry R1-8), as we increase the value of θ from 1 to 8 degrees, this also increase the ramp 1 length which cause a longer shockwave 1 that in turns capture more air as compared to standard model and at last increases the stagnation pressure ratio.

From our observations we have concluded that R2-18 and R1-8_R-18 are not performing anywhere close to the other 2 models. Despite of the fact that for the blue region and green region values of all the 4 models are almost equal or vary by a small margin, but because in the last 2 model the cowl portion has become parallel to the closing end of the ramp 2 or has moved ahead of it can be clearly seen in the following figures (pressure plot for R1-8_R-18 and pressure plot for R2-18).Due to this reason, we cannot see the formation of 3rd shockwave in these models which is very much necessary for the final air to enter the inlet and then move on to isolator region. This shockwave is necessary because this cause the air stream to become parallel to the inlet and thus having a straight path.

International Journal of Advances in Engineering and Management (IJAEM)
Volume 4, Issue 5 May 2022, pp: 2243-2258 www.ijaem.net ISSN: 2395-5252

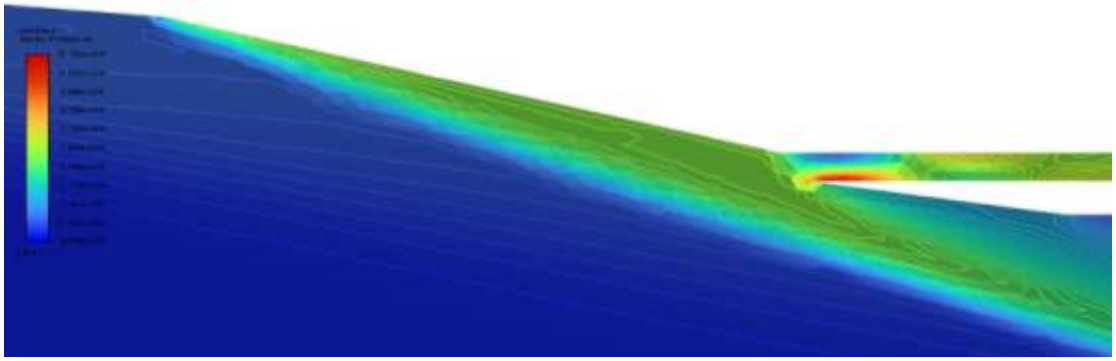

Pressure plot for R1-8_R-18

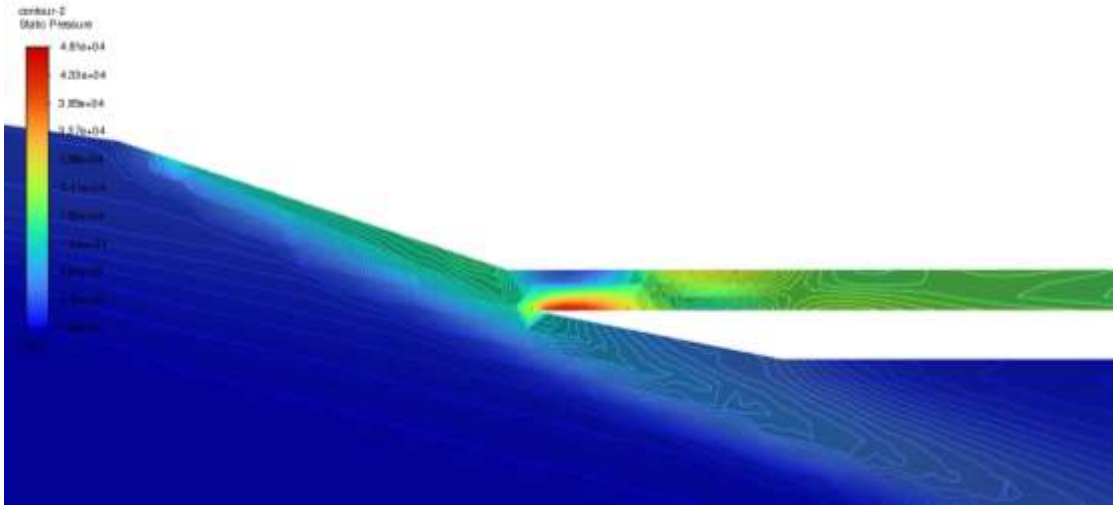

Pressure plot for R2-18

VI. MACH PLOT

XY Mach plot

International Journal of Advances in Engineering and Management (IJAEM)
Volume 4, Issue 5 May 2022, pp: 2243-2258 www.ijaem.net ISSN: 2395-5252

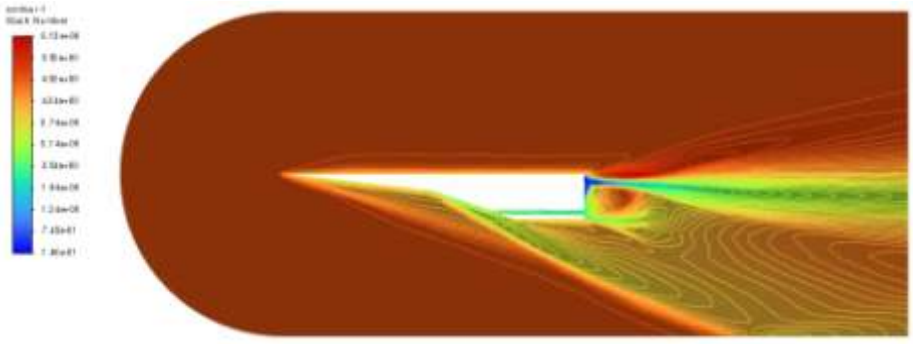

R2-18 Mach contour line plot

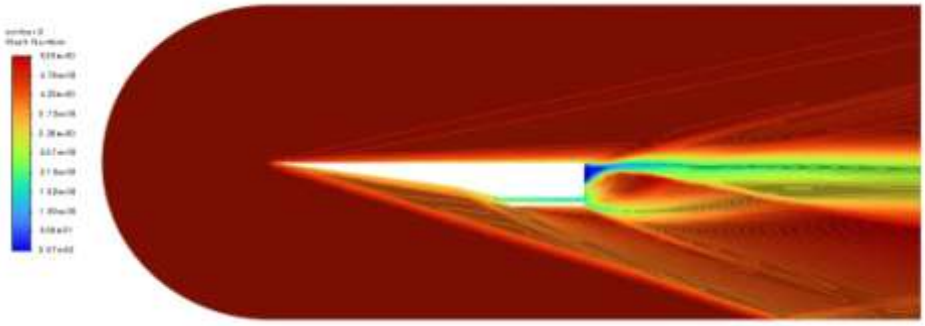

R1-8Machcontourlineplot

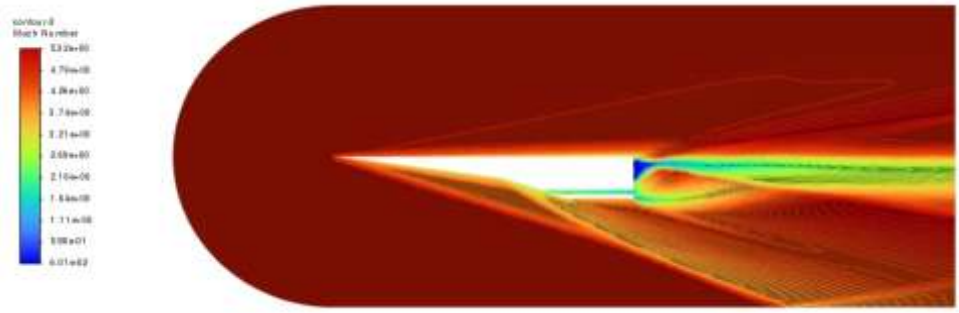

R1-8_R2-18 Mach contour line plot

VII. PRESSURE CONTOUR PLOT

XYPressurecontour lineplot

International Journal of Advances in Engineering and Management (IJAEM)
Volume 4, Issue 5 May 2022, pp: 2243-2258 www.ijaem.net ISSN: 2395-5252

R1-8 Pressurecontour lineplot

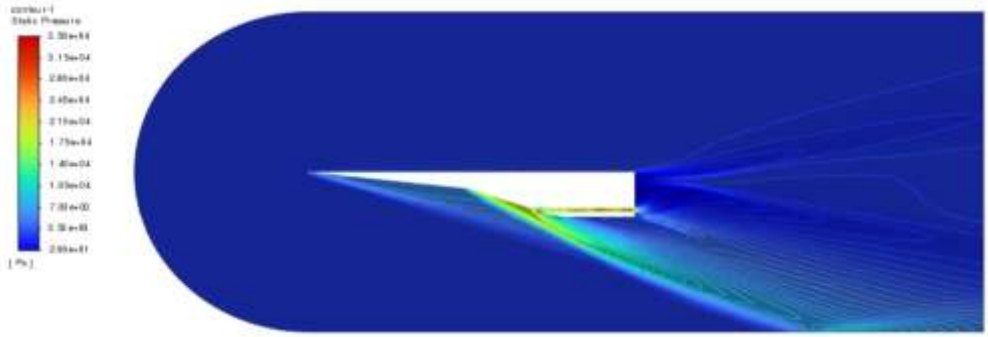

R2-18Pressurecontourlineplot.

R1-8_R2-18Pressure contour lineplot

VIII. TEMPERATURE CONTOUR PLOT

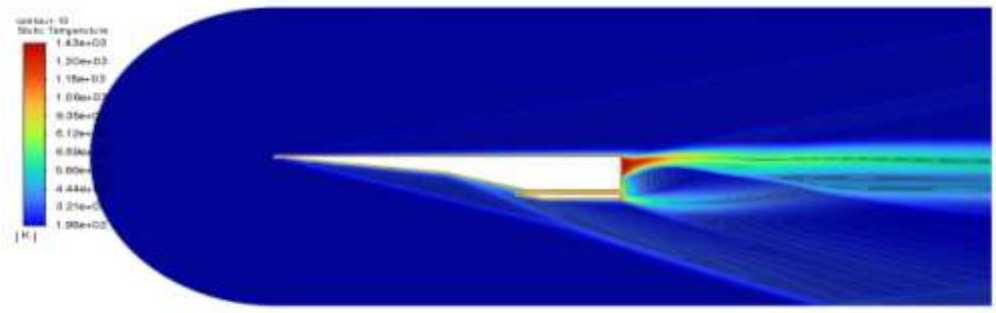

XY Temperaturecontour lineplot

International Journal of Advances in Engineering and Management (IJAEM)
Volume 4, Issue 5 May 2022, pp: 2243-2258 www.ijaem.net ISSN: 2395-5252

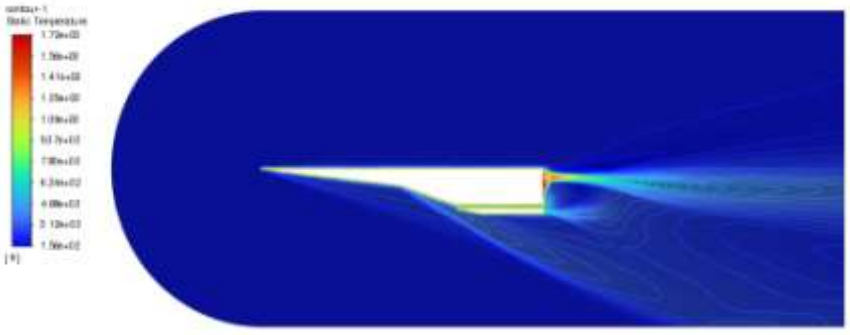

R2-18 Temperature contourlineplot.

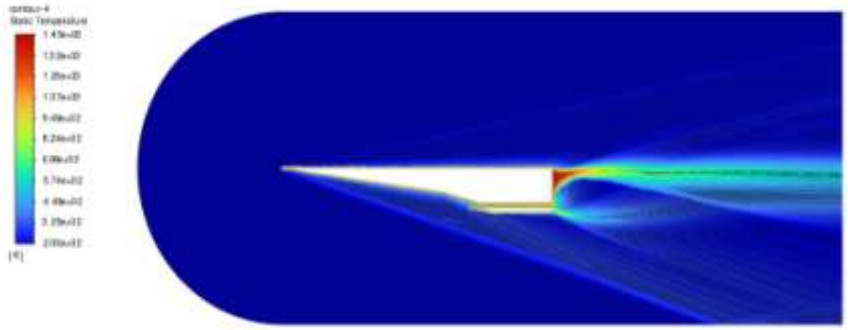

R1-8Temperature contourlineplot

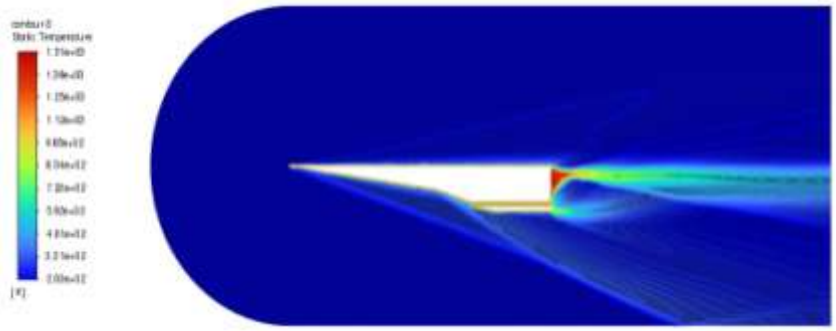

R1-8_R2-18Temperature contour lineplot

IX. CONCLUSION

From this study we can conclude that, while designing inlet geometry for double ramp Scramjet. The following things must be kept in mind. Firstly, the Ramp 1 can be made longer as compared to ramp 2 and should have smaller ramp angle, otherwise air will get blocked. Secondly, on increasing the ramp length it also increases the length of the shockwave 1 and this cause more air to get trapped in it. Third and the most important conclusion is that we cannot let the cowl to pass over the ramp 2 ending edge as the model showcased in the last 2 models. Thus, we can say that if we want to adjust the amount of into the inlet by ourselves then we need to develop some sort of mechanism in which we can adjust the cowl length.

X. ADVANTAGES AND APPLICATION

This numerical study will help us understand the how much variation are possible in the ramp angle, plus how side wall reacts to the hypersonic flow.

All these talks will give an idea as to how much variation is possible in the design of these Scramjet engines. Now because there are only 4 major components that are present in a Scramjet engine, which are inlet, isolator and combustion chamber and nozzle. Out of which design of nozzle and combustion chamber are generally fixed so we are left up with the inlet in which we can do the design changes.

Some advantages are:

1. The study will help us design better Scramjet engine
2. Give us a greater understanding the Mach number on which these engines work the best.
3. Opens door for better design and new designs.

REFERENCES

[1]. Shock Induced Separating Flows in Scramjet Intakes. Yao, D. Rincon, and Y. Zheng.

[2]. Nguyen, T., Behr, M., and Reinartz, B., "Numerical Investigation of Compressible Turbulent Boundary Layer Overexpansion Corner," AIAA Paper 2009-7371(2009).

[3]. M. Krause, M. Behr, and J. Ballmann, AIAA Paper, 2008-2598 (2008).

[4]. ANSYS v12 manual, ANSYS Ltd. (2009).

[5]. Haberle, J. and Gulhan, A., "Investigation of Two-Dimensional Scramjet Inlet Flowed at Mach 7," Journal of Propulsionand Power, Vol. 24, No. 3, 2008, pp. 446-459.

[6]. Bramkamp, F. D., Lamby, P., and Muller, S., "An adaptive multiscale finite volume solver for unsteady and steady on computations," Journal of Computational Physics, Vol. 197, 2004, pp. 460-490.

[7]. Krause, M. and Ballmann, J., "Enhanced Design of a Scramjet Intake Using Two Dierent RANS Solvers," 26th Inter-national Symposium on Shock Waves, Goettingen, Germany, 15-20 July 2007, 2007, pp. 589-594.55.